

## Source Mechanisms of Harmonic Tremors at Sakurajima Volcano

Takeshi TAMEGURI\*, Sukir MARYANTO\*\* and Masato IGUCHI\*

(Received, November 21, 2006; Accepted, August 21, 2007)

Source mechanisms of harmonic tremors observed after B-type earthquake swarm (HTB) and those immediately after explosive eruption (HTE) at Sakurajima are estimated by inversion of root mean square (RMS) seismic amplitudes of 3 components at 5 stations. HTB and HTE had a similar source mechanism that indicates isotropic components of more than 50%. Source depths of the HTB and HTE correspond to the location of a gas pocket formed at uppermost part of the conduit. We infer that HTB is generated by resonance of the gas pocket formed after swarm of B-type earthquake and that HTE is related with resonance of the gas pocket of which top is partially collapsed by the explosion.

**Key words:** harmonic tremor, moment tensor, Sakurajima volcano

## 1. Introduction

Eruptive activity with Vulcanian style has continued at the summit crater, Minamidake of Sakurajima since 1955. Harmonic tremor (C-type tremor) have been observed in active eruptive stages at Sakurajima volcano (Kamo *et al.*, 1977; Nishi, 1984), and are characterized by regular peaks of spectra, composed of fundamental frequency and its overtones from analyses of spectrum and particle motion (e.g. Kakuta and Idegami, 1970; Kamo *et al.*, 1977). As a result, the harmonic tremors are classified into two types. One is the tremors observed several hours after B-type earthquake swarm (HTB) and the other is the tremors observed a few minutes after explosive eruption (HTE). Peak frequencies of HTB are constant in duration of vibration. In contrast, those of HTE gradually increase (Maryanto *et al.*, 2005). During 1982–2002, 993 HTBs occurred and only 5 HTEs were recorded. HTEs were rare harmonic tremor at Sakurajima volcano.

Mechanisms of harmonic tremors have been investigated by analyses of spectra at other volcanoes. Harmonic tremor at Semeru volcano was caused by repetitive triggering sources at shallow part (Schlindwein *et al.*, 1995). Hellweg (2000) proposed that harmonic tremor at Lascar volcano was excited by movement of water and gases near the surface. These studies discussed mechanisms on regular repetition of triggering source for harmonic tremors; however source mechanism of the trigger source has not been investigated. Radiation pattern or moment tensor of the harmonic

tremors were also practically not reported. And also, their source locations were inferred at shallow parts near the surface, but the depths were not quantitatively determined in the previous studies. Maryanto *et al.* (2005) indicated that Rayleigh waves were dominant in harmonic tremors at Sakurajima volcano from analyses of particle motion.

In this study, we estimate moment tensor and source depths of the two kinds of harmonic tremors, HTB and HTE, at Sakurajima volcano from spatial distributions of RMS seismic amplitudes. We further discuss common and different factors in their source mechanisms.

## 2. Data

Seismograms at 5 stations ranging 1.7–4.4 km from the active crater (Fig. 1) are used for analyses. At 4 stations, three-component short-period seismometers (natural period  $T_0=1$  s, damping constant  $h=1.0$ ) are installed in boreholes at depths of 85 to 290 m. Station HIK is equipped with the seismometers installed on the surface in vaults. One horizontal component seismometer is set parallel to the direction from the station to the summit crater (longitudinal component) and the other is set perpendicular to the direction (tangential component). Velocity seismograms recorded before 2001 were digitized with an A/D resolution of 12 bit and a sampling rate of 200 Hz from analog magnetic tapes. Seismic signals recorded after 2001 were recorded with an A/D resolution of 22 bit and a sampling rate of 200 Hz.

\* Sakurajima Volcano Research Center, Disaster Prevention Research Institute, Kyoto University, Sakurajima-Yokoyama, Kagoshima 891–1419, Japan.

\*\* Department of Physics, Faculty of Science, Brawijaya

University, Jln. Veteran 11, Malang, Indonesia.

Corresponding author: Takeshi Tameguri  
e-mail: tameguri@svo.dpri.kyoto-u.ac.jp

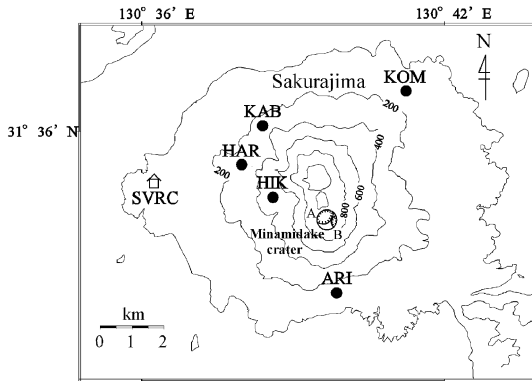


Fig. 1. Location of seismic stations. Solid circles denote stations used for analyses. SVRC means Sakurajima Volcano Research Center.

Figure 2 shows examples of waveforms at HTB and HTE. We analyzed 1 minute records (16 h 12 m 15 s–16 h 13 m 15 s) of HTB on July 20, 1990, which continued about 2 hours from 14 h (JST), and 6 minute records of HTE that started at 11 h 19 m following an explosive eruption occurred on 11 h 15 m on October 11, The HTE continued for 12 minutes.

Waveforms of the HTB and HTE observed at 5 stations are shown in Fig. 3. The HTB and HTE have the largest amplitudes at station HIK, the closest station to the crater. Amplitudes decrease with distance from the crater. The amplitudes of horizontal component are larger than those of vertical component and longitudinal components have the largest amplitudes, except station KOM.

Spectra calculated for 10 seconds records of the HTB and HTE at station HIK are shown in Fig. 4. The spectra of HTB have clear dominant peaks at 1.6 Hz, 3.2 Hz, 4.8 Hz, 6.4 Hz and 8.0 Hz. The peak at 1.6 Hz is fundamental mode the others are its overtones. Dominant peaks of the spectra of HTE appear at 1.6 Hz, 3.2 Hz, 4.8 Hz, 6.4 Hz, and 8.0 Hz. Waveforms processed by band-pass filter with a band width of  $\pm 0.05$  Hz of fundamental ( $f_1$ ) and second mode ( $f_2$ ) at station HIK are shown in Fig. 5. The amplitudes of vertical components of HTB and HTE are almost stable. Wave trains with spindle shape of duration of a few to 10 seconds appear in horizontal components. The amplitudes of the fundamental mode of HTE are larger than those of the second mode. In contrast, the amplitudes of the second mode of HTB are larger than those of the fundamental mode. The HTB may be generated by a source which has two fundamental frequencies of  $f_1$  and  $f_2$ .

### 3. Analysis

Moment tensor solution of the harmonic tremors are

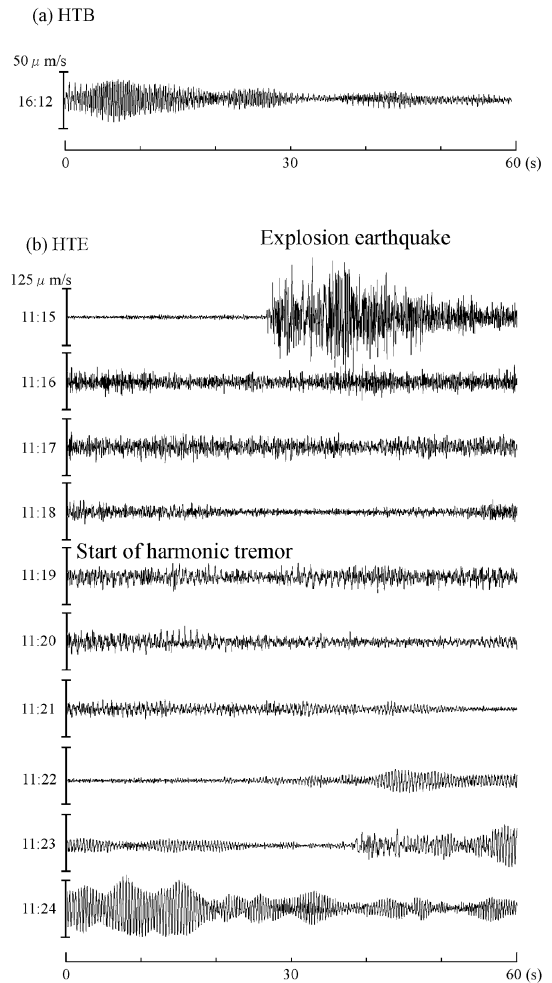


Fig. 2. Seismograms of harmonic tremors. The seismograms are observed by a vertical component of seismometer at station HIK. (a) HTB occurred on July 20, 1990. (b) Explosion earthquake occurred at 11: 15 on October 11, 2002 and HTE started at 11: 19.

estimated by inversion of RMS amplitudes of 4 s time window, because it is difficult to detect common phases of harmonic tremors among the 5 stations and it is impossible to apply a conventional waveform inversion method to obtain the moment tensor. By using the data of RMS amplitudes, we can evaluate an average moment tensor solution for the given window. Here, fundamental and second modes of harmonic tremors are analyzed, because amplitudes of higher mode are small at far stations from the crater. Peak frequencies of the fundamental and second modes of HTB are nearly constant. RMS amplitudes are calculated from seismograms band-pass filtered by 1.55–1.65 Hz ( $f_1$ ) and

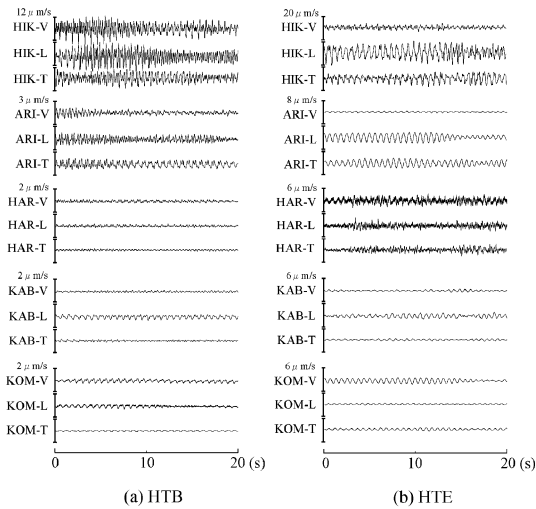


Fig. 3. Examples of 3-component velocity waveforms of harmonic tremors at 5 stations. (a) HTB from 16: 12: 55 to 16: 13: 15 on July 20, 1990. (b) HTE from 11: 21: 00 to 11: 21: 20 on October 11, 2002.

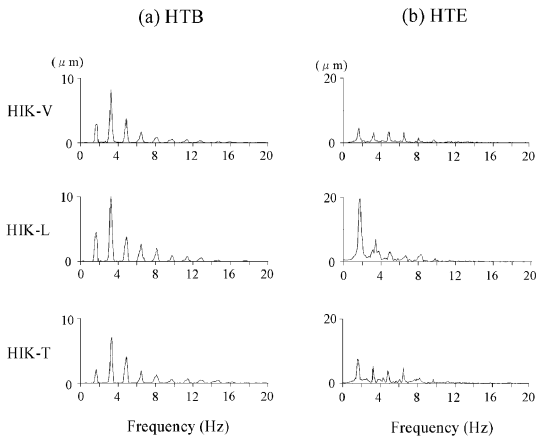


Fig. 4. Spectra of harmonic tremors. The spectra were obtained from 10s-seismograms at station HIK shown in Fig. 3. (a) Spectra of HTB from 16: 12: 55. (b) Spectra of HTE from 11: 21: 00.

those filtered by 3.15–3.25 Hz ( $f_2$ ) for HTB. Fundamental frequency of HTE increased 1.0 to 2.6 Hz in time window of analysis. So, center frequency of band-pass filter with band width of  $\pm 0.05$  Hz is changed corresponding to dominant peak frequencies. In order to remove local site effect at each station, the waveform amplitudes were corrected by a site amplification factor, which is defined as the average of ampli-

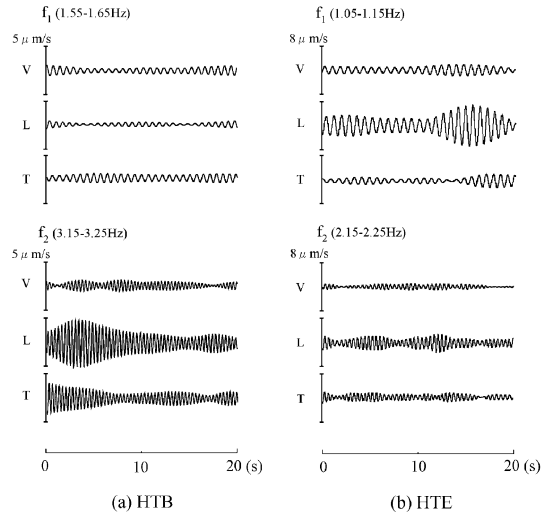


Fig. 5. Examples of waveform band-pass filtered at  $f_1$  and  $f_2$  with band width of  $\pm 0.05$  Hz. Seismograms are observed at station HIK. (a) HTB from 16: 12: 55 to 16: 13: 15 on July 20, 1990. (b) HTE from 11: 19: 00 to 11: 19: 20 on October 11, 2002.

tude ratio of teleseismic earthquakes with frequencies of 1–3 Hz. The site correction factors, which are the inverse of the amplification factors, at stations HIK, ARI, HAR and KAB referring to KOM are 0.95, 0.64, 1.48 and 0.86, respectively.

We modified the waveform inversion method (Kikuchi and Kanamori, 1991) so as to use RMS amplitudes. Green's functions to reproduce synthetic waveforms are calculated by the method of Hisada (1994). The depths of seismometer are taken into account in the calculation. A homogeneous half-space with  $V_p = 2.5$  km/s,  $V_s = 1.44$  km/s, and a density of  $2.5 \times 10^3$  kg/m<sup>3</sup> (Iguchi, 1994) is assumed to calculate the Green's functions. Synthetic RMS amplitudes are calculated from synthetic waveforms predicted from sinusoidal source time functions with frequencies of the fundamental and second modes. The synthetic waves are band-pass filtered with the same frequency bands as the observed waveforms. It is assumed that epicenter of harmonic tremor is the summit crater, because amplitudes of HTB and HTE are the largest at station HIK, which is the closest station to the crater (Fig. 3). The moment tensor inversion is conducted for 4 cases of source depths: 2.0, 1.0, 0.5 and 0.3 km. In this analysis, RMS amplitudes are obtained in 4 s windows. In order to confirm validity of the length of time window, we test the inversion method in case of 2 s and 8 s time windows. Similar results are obtained to those of 4 s window.

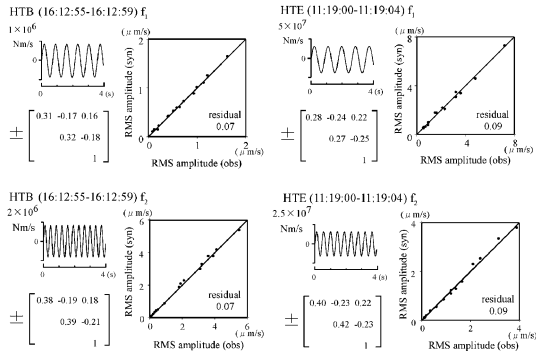


Fig. 6. Examples of results of the inversion. Assumed source time function and obtained moment tensor components are shown in left side. Fitness of synthetic RMS amplitudes to observed ones are plotted in right side. (a) Fundamental frequency of HTB. (b) Second mode of HTB. (c) Fundamental frequency of HTE. (b) Second mode of HTE.

#### 4. Results

Examples of inversion results are shown in Fig. 6. Result for  $f_1$  of HTB shows that a vertical dipole is dominant, non-diagonal components are 20% of  $M_{zz}$  component, and diagonal components have same polarity. These represent a volume change of the source. Moment tensor solution for  $f_2$  of HTB is similar to that of  $f_1$ . Peak to peak amplitude of the moment rates for  $f_1$  and  $f_2$  are  $1.8 \times 10^6$  Nm/s and  $3.8 \times 10^6$  Nm/s, respectively. Synthetic RMS amplitudes assuming source depth of 0.5 km are best fitted to the observed ones with a residual of 0.07. Result for  $f_1$  of HTE is almost same as that of HTB, indicating dominant vertical dipole and diagonal components with a same polarity. Non-diagonal components are 25% of  $M_{zz}$  component. Moment tensor solution for  $f_2$  of HTE are similar to that of  $f_1$ . Peak to peak amplitude of the moment rates for  $f_1$  and  $f_2$  are  $0.7 \times 10^8$  Nm/s and  $0.3 \times 10^8$  Nm/s, respectively. Source depth of 0.3 km gives the best result.

Next, moment tensor components are decomposed to isotropic, compensated linear vector dipole (CLVD; Knopoff and Randall, 1970), and double couple (DC) parts using the method of Horálek *et al.* (2002), and temporal changes of the three parts and moment-rates are investigated (Fig. 7). Isotropic components for  $f_1$  of HTB are 50–60%, and CLVD and DC components are about 20%. The three components for  $f_2$  are about 60%, 20–30%, and 10%, respectively. Moment-rates for  $f_1$  fluctuate, ranging from  $3.2 \times 10^6$  to  $4.1 \times 10^6$  Nm/s and moment-rates for  $f_2$  decrease from  $9.5 \times 10^6$  Nm/s in the same analysis window. Isotropic components for  $f_1$  of HTE are 50–70%, and CLVD and DC components

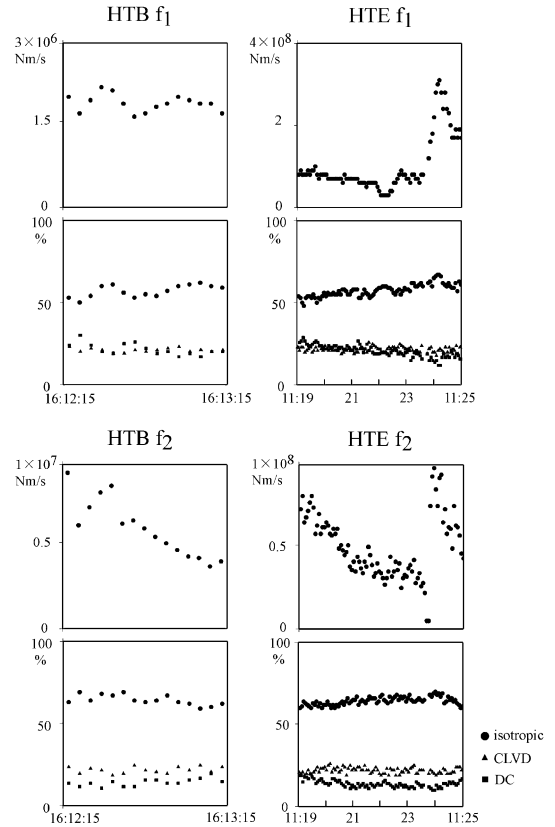


Fig. 7. Moment-rate and moment tensor components. Circles, triangles, and squares represent percentages of isotropic, CLVD, and DC components of moment tensor, respectively. (a) Fundamental frequency of HTB. (b) Second mode of HTB. (c) Fundamental frequency of HTE. (b) Second mode of HTE.

are about 20% and 10–20%, respectively. The three components for  $f_2$  are about 60%, 20–30%, and 10%, respectively. Moment-rates for  $f_1$  are stable until 11h23m, ranging  $0.6 \times 10^8$  to  $0.9 \times 10^8$  Nm/s and increased to  $2.4 \times 10^8$ – $3.1 \times 10^8$  Nm/s from 11 h 24 m. Moment-rates for  $f_2$  range from  $0.5 \times 10^7$  to  $9.5 \times 10^7$  Nm/s. Although the moment-rates change in the analysis window, a ratio of the three parts is stable.

Source depths of HTB and HTE are estimated to be 0.5 km and 0.3 km, respectively, beneath the crater in all analysis windows. In order to examine the accuracy of the estimated source depths, moment tensor inversions are done for source depths ranging from 0.1 km to 2.0 km with increment of 0.1 km, using the seismograms of HTB at 16 h 12 m 55 s and HTE at 11 h 21 m 00 s. The source depths of HTB and HTE as minimizing the residual between observed RMS amplitude and synthet-

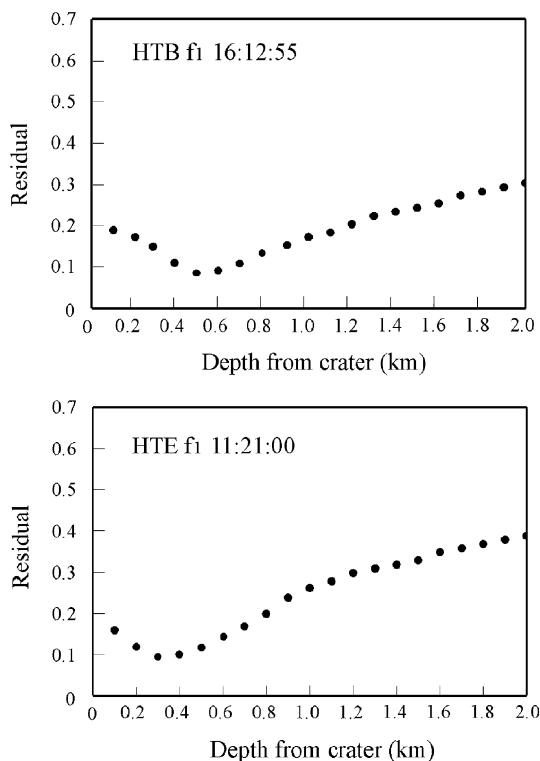


Fig. 8. Residuals of RMS amplitudes between observed and synthetics plotted against source depths. Upper and lower figures are HTB and HTE, respectively.

ic one are estimated to be 0.5 km and 0.3 km, respectively (Fig. 8). The shallow source depths are appropriate, because local minimum in residuals is not recognized and amplitudes of body wave are small (Maryanto *et al.*, 2005).

## 5. Discussion

Moment tensors of HTB and HTE at Sakurajima volcano include isotropic component more than 50%. This indicates that the harmonic tremors are excited by repetition of expansion and contraction of the source. CLVD component having a vertical main axis is included by 20% in moment tensor. The source repeating expansion and contraction is dominated by vertical dipole, as shown by dominant  $M_{zz}$  component. We infer that the source of harmonic tremor is related to vertically dominated volume change of fluid.

Source depths of HTB and HTE are estimated to be 0.5 km and 0.3 km, respectively. The depths correspond to the location of a gas pocket that are inferred from tilt and strain steps caused by an instantaneous pressure decrease reflecting the outbreak of a gas pocket at 0.5 km beneath the crater (Ishihara, 1990). The depths

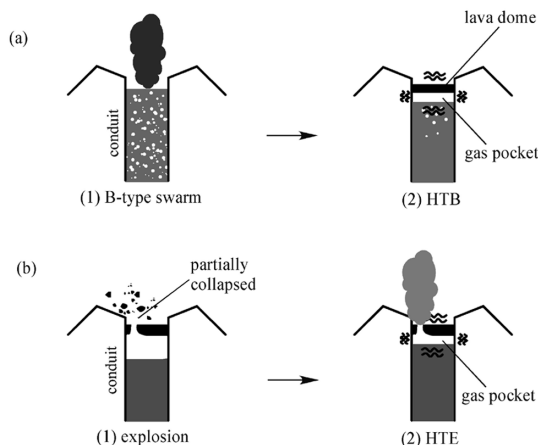


Fig. 9. Conceptual models of HTB and HTE. (a) HTB. 1) Volcanic conduit is filled with magma including gas during B-type earthquake swarm. 2) The magma reaching crater bottom becomes solidified lava dome by cooling and a gas pocket is formed beneath the lava dome. HTB is generated by resonance of the gas pocket. (b) HTE. 1) An explosion occurs, partially collapsing the lava dome. 2) HTE is generated by resonance of gas pocket during gas release from small vent of the lava dome.

are also consistent with the location of the source of long-period largest motion for explosion earthquakes (Tameguri *et al.*, 2002).

Figure 9 shows the conceptual models of HTB and HTE. Generating B-type earthquakes, magma ascends to the crater bottom and fills the conduit (Iguchi 1994; Fig. 9a-1). The magma reaching to crater bottom forms a lava dome, which is a magma solidified by cooling from the surface. When gas is released from magma beneath the lava dome, a gas pocket can be formed at uppermost part of conduit (Ishihara, 1985). It is considered that harmonic tremor is generated by resonance of fluid with boundary of large contrast of impedance (Kamo *et al.*, 1977; Fujita and Ida, 2003). We infer that HTB after swarm of B-type earthquakes is generated by resonance of the gas pocket formed at uppermost part of conduit (Fig. 9a-2). During the occurrence of HTB, we observed weak gas emission from crater which may play a role in driving source for generation of the HTB. On the other hand, HTE occurs a few minutes after explosive eruption (Maryanto *et al.*, 2005), indicating that the gas pocket sealed by lava dome is broken by an explosion (Ishihara, 1985; Tameguri *et al.*, 2002). If the gas pocket trapped beneath the crater is the resonance source generating harmonic tremor, the harmonic tremor would not occur

after explosions. However, if the lava dome above the gas pocket is not completely destroyed (Fig. 9b-1), and volcanic gas is released from a hole smaller than the size of gas pocket, the gas pocket that has a large impedance contrast to the surrounding volcanic edifice may play a role of the resonator (Fig. 9b-2). Increase in peak frequencies of the HTE may be caused by decrease of volume of the gas pocket that is introduced by slow gas release from the small hole after the explosion. The moment-rates of HTE suddenly became large at 11 h 23 m 40 s (Fig. 7) when a seismic event similar to a B-type earthquake occurred at this time as shown in Fig. 2. This correlation suggests that resonance of the gas pocket is excited by a seismic event. It is inferred that HTB and HTE are excited by resonance of the same gas pocket formed before an explosion, because the moment tensor solutions of HTB and HTE are almost same.

The moment tensor solutions are dominated by vertical dipole ( $M_{zz}$ ). The sources of harmonic tremors are approximated by vertical vibration of a horizontally extended thin source. Furthermore, the harmonic tremor is characterized by regular peaks of spectra, composed of fundamental frequency and its overtones. Fujita and Ida (2003) showed that the characteristics of regular peaks of spectra are caused by resonance of planar inclusion. So, it is inferred that the source of harmonic tremors is formed in a thin plane filled with gas between a lower part of the lava dome and the top of magma in the conduit.

## 6. Conclusions

The HTB and HTE show a same moment tensor solution dominated by vertical dipole, and the source is characterized by repeating expansion and contraction. The sources of harmonic tremors are approximated by vertical vibration of a horizontally extended thin source. Source depths of 0.3–0.5 km coincide with the depth of gas pocket that inferred to be formed beneath the crater. We suggest that the harmonic tremors are generated by resonance of the gas pocket.

## Acknowledgement

We greatly thank the staffs of Sakurajima Volcano Research Center, Disaster Prevention Research Institute, Kyoto University, for maintenance of the observation system. We thank Dr. Takeshi Nishimura of Tohoku University for discussion about the source mechanism. Comments by Dr. Eisuke Fujita of National Research Institute for Earth Science and Disaster Prevention, Dr. Haruhisa Nakamichi of Nagoya University, and Dr. Tomoki Tsutsui of Akita University were very helpful to revise the manuscript.

## References

- Fujita, E. and Ida, Y. (2003) Geometrical effects and low-attenuation resonance of volcanic fluid inclusions for the source mechanism of long-period earthquakes. *J. Geophys. Res.*, **108**, 2118, 10.1029/2002 JB001806.
- Hellweg, M. (2000) Physical model for the source of Lascar's harmonic tremor. *J. Volcanol. Geotherm. Res.*, **101**, 183–198.
- Hisada, Y. (1994) An efficient method for computing Green's functions for a layered half-space with sources and receivers at close depths. *Bull. Seism. Soc. Am.*, **84**, 1456–1472.
- Horálek, J., Šílený, J. and Fischer, T. (2002) Moment tensors of the January 1997 earthquake swarm in NW Bohemia (Czech Republic): double-couple vs. non-double-couple events. *Tectonophysics*, **356**, 65–85.
- Iguchi, M. (1994) A vertical expansion source model for the mechanism of earthquakes originated in the magma conduit of andesitic volcano, Sakurajima, Japan. *Bull. Volcanol. Soc. Japan*, **39**, 49–67.
- Ishihara, K. (1985) Dynamical analysis of volcanic explosion. *J. Geodynamics*, **3**, 327–349.
- Ishihara, K. (1990) Pressure sources and induced ground deformation associated with explosive eruptions at an andesitic volcano: Sakurajima volcano, Japan. In *Magma transport and storage* (Ryan, M. P. ed), John Wiley & Sons, Chichester, 333–356.
- Kakuta, T. and Idegami, Z. (1970) The volcanic tremors of "C-type" at the Sakurajima volcano. *Bull. Volcanol. Soc. Japan*, **15**, 61–74 (Japanese with English abstract).
- Kamo, K., Furuzawa, T. and Akamatsu, J. (1977) Some natures of volcanic micro-tremors at the Sakurajima volcano. *Bull. Volcanol. Soc. Japan*, **22**, 41–58 (Japanese with English abstract).
- Kikuchi, M. and Kanamori, H. (1991) Inversion of complex body waves-III. *Bull. Seism. Soc. Am.*, **81**, 2335–2350.
- Maryanto, S., Iguchi, M. and Tameguri, T. (2005) Spatio-temporal characteristics on spectra and particle motion of harmonic tremors at Sakurajima volcano, Japan. *Ann. Disast. Prev. Res. Inst.*, **48B**, 329–339.
- Nishi, K. (1984) Volcanic B-type earthquake swarm preceding volcanic explosion. *Ann. Disast. Prev. Res. Inst.*, **27B-1**, 29–34 (Japanese with English abstract).
- Knopoff, L. and Randall, M.J. (1970) The compensated linear-vector dipole: a possible mechanism for deep earthquakes. *J. Geophys. Res.*, **75**, 4957–4963.
- Schindwein, V., Wassermann, J. and Scherbaum, F. (1995) Spectral analysis of harmonic tremor signals at Mt. Semeru volcano, Indonesia. *Geophys. Res. Lett.*, **22**, 1685–1688.
- Tameguri, T., Iguchi, M. and Ishihara, K. (2002) Mechanism of explosive eruptions from moment tensor analyses of explosion earthquakes at Sakurajima volcano. *Bull. Volcanol. Soc. Japan*, **47**, 197–215.

## 桜島火山におけるハーモニック微動の震源メカニズム

為栗 健・S. Maryanto・井口正人

桜島火山において発生するハーモニック微動のモーメントテンソル解析を行った。B型地震群発後に発生する微動(HTB)と爆発的噴火直後に発生する微動(HTE)のモーメントテンソル成分に大きな違いはなく、等方成分は50%以上、CLVD成分は20~30%、DC成分は20%以下であった。鉛直方向のダイポール成分が大きく、鉛直方向の力が優勢な震源が推定される。震源は火口直下の浅部であり、爆発的噴火発生前に火口底直下に形成されているガス溜まりが微動の発生に関与していると考えられる。